[CANCER RESEARCH 64, 7426–7431, October 15, 2004]

HIV-1 Protease Inhibitor, Ritonavir: A Potent Inhibitor of CYP3A4, Enhanced the Anticancer Effects of Docetaxel in Androgen-Independent Prostate Cancer Cells *In vitro* and *In vivo*

Takayuki Ikezoe,[1,3] Yasuko Hisatake,[1] Tamotsu Takeuchi,[4] Yuji Ohtsuki,[4] Yang Yang,[3] Jonathan W. Said,[2] Hirokuni Taguchi,[3] and H. Phillip Koeffler[1]

[1]Division of Hematology/Oncology, Cedars-Sinai Medical Center and UCLA School of Medicine, Los Angeles, California; [2]Department of Pathology, Center for Health Science, UCLA School of Medicine, Los Angeles, California; and Departments of [3]Internal Medicine and [4]Tumor Pathology, KMS, Kochi University, Kochi, Japan

ABSTRACT

We previously showed that HIV-1 protease inhibitors (PIs) slowed the proliferation of human myeloid leukemia cells and enhanced their differentiation in the presence of all–*trans*-retinoic acid. In this study, we found that PIs, including ritonavir, saquinavir, and indinavir, inhibited the growth of DU145 and PC-3 androgen-independent prostate cancer cells as measured by a clonal proliferation assay. Recent studies showed that ritonavir inhibited cytochrome P450 3A4 enzyme (CYP3A4) in liver microsomes. The CYP3A4 is involved in drug metabolism and acquisition of drug resistance. To clarify the drug interaction between ritonavir and other anticancer drugs, we cultured DU145 cells with docetaxel either alone or in combination with ritonavir. Ritonavir enhanced the antiproliferative and proapoptotic effects of docetaxel in the hormonally independent DU145 prostate cancer cells *in vitro* as measured by the clonogenic soft agar assay and detection of the activated form of caspase-3 and cleavage of poly(ADP-ribose) polymerase using Western blot analysis. Real-time PCR showed that docetaxel induced the expression of *CYP3A4* at the transcriptional level, and ritonavir (10^{-5} mol/L) completely blocked this induction. An ELISA-based assay also showed that ritonavir inhibited DNA binding activity of nuclear factor κB (NFκB) in DU145 cells, which is a contributor to drug resistance in cancer cells. Furthermore, combination treatment of docetaxel and ritonavir dramatically inhibited the growth of DU145 cells present as tumor xenografts in BNX nude mice compared with either drug alone. Importantly, docetaxel induced expression of *CYP3A4* in DU145 xenografts, and ritonavir completely blocked this induction. Ritonavir also inhibited NFκB DNA binding activity in DU145 xenografts. Extensive histologic analyses of the liver, spleen, kidneys, bone marrow, skin, and subcutaneous fat pads from these mice showed no abnormalities. In summary, combination therapy of ritonavir and anticancer drugs holds promise for the treatment of individuals with advanced, drug resistant cancers.

INTRODUCTION

Treatment of androgen-independent prostate cancer (AIPC) remains unsatisfactory, even though new anticancer drugs have been developed. One of the promising chemotherapeutic treatments for individuals with AIPC is docetaxel, which has anti–prostate cancer effects in ~40% of individuals with AIPC (1–3).

HIV-1 protease inhibitors (PIs) have become important tools in the management of HIV infection; these include saquinavir mesylate, ritonavir, and indinavir sulfate. Recent studies showed that PIs possess antitumor activity, which is independent from their ability to inhibit HIV protease. We previously found that saquinavir, ritonavir, and indinavir induced growth arrest and differentiation of NB4 and HL-60 human myelocytic leukemia cells and enhanced the ability of all–*trans*-retinoic acid (ATRA) to decrease proliferation and increase differentiation of these cells (4). Other investigators have shown that PIs can decrease proliferation of Kaposi's sarcoma and prostate cancer cells via inhibition of nuclear factor κB (NFκB) activity (5–7). We also have recently found that PIs induced growth arrest and apoptosis of multiple myeloma cells via inhibition of signal transducers and activators of transcription 3 and extracellular signal-regulated kinase 1/2 signaling (8).

PIs are metabolized by cytochrome P450 3A4 (CYP3A4) in liver microsomes (9). Interestingly, among the PIs, only ritonavir showed strong CYP3A4 inhibitory effects. Noting this activity, investigators have coadministered ritonavir with saquinavir and found markedly elevated and sustained plasma levels of saquinavir in rat and dog models. This occurred, supposedly, by inhibiting metabolism of saquinavir (10), and this combination is clinically used for individuals with HIV infection (11). On the basis of the pharmacokinetics of ritonavir, a coformulated agent containing lopinavir and ritonavir has been developed: Low doses of ritonavir enhanced the activity of lopinavir (12), and this formulation is being used for first-line therapy for some HIV-infected individuals. Collectively, we hypothesized that ritonavir might enhance the antitumor activity of docetaxel, the latter being a substrate for CYP3A4 (13). In this study, we found that ritonavir, saquinavir, and indinavir inhibited the growth of the DU145 and PC-3 AIPC cells as measured by the clonogenic assay. Ritonavir blocked the docetaxel-induced expression of *CYP3A4* at the mRNA level in DU145 cells and enhanced the antitumor effect of docetaxel *in vitro* and in BNX nude mice bearing DU145 tumors.

MATERIALS AND METHODS

Cell Lines. PC-3 and DU145 cells were obtained from the American Type Culture Collection (Manassas, VA) and were grown in either RPMI 1640 medium (Life Technologies, Inc., Rockville, MD) with 10% heat-inactivated fetal bovine serum (FBS; Life Technologies, Inc.) or DMEM (Life Technologies, Inc.) with 10% FBS, respectively.

Chemicals. Saquinavir mesylate (Roche, Basel, Switzerland), ritonavir (Abbott Labs, North Chicago, IL), and indinavir sulfate (Merck, West Point, PA) were dissolved in dimethyl sulfoxide (Burdick & Jackson, Muskegon, MI) to a stock concentration of 10^{-2} mol/L and stored at −80°C. Docetaxel (Aventis Pharmaceuticals Inc., Tokyo, Japan) was dissolved in PBS to a stock concentration of 10^{-4} mol/L and stored at 4°C.

Colony-Forming Assay. DU145 and PC-3 cells were cultured in a two-layer soft agar system for 14 days as described previously (4). Washed single-cell suspensions of cells were enumerated and plated into 24-well flat-bottomed plates with a total of 500 cells/well in a volume of 400 μL/well. The feeder layer was prepared with agar that had been equilibrated at 42°C. Before this step, PIs were pipetted into the wells. After incubation for 14 days, colonies were counted. All of the experiments were done three times using triplicate plates per experimental point.

RNA Isolation and Reverse Transcription-PCR. Total RNA was isolated as described previously using TRIzol (Life Technologies, Inc.; ref. 4).

Received 8/27/03; revised 7/21/04; accepted 8/11/04.

Grant support: NIH, including AT00151 the UCLA Center for Dietary Supplements Research: Botanicals, and also in part by the Parker Hughes Fund and the Aaron Eschman Fund. H. P. Koeffler is a member of University of California-Los Angeles Jonsson Comprehensive Cancer Center and Molecular Biology Institute and holds an endowed Mark Goodson Chair of Oncology Research at Cedars-Sinai Medical Center.

The costs of publication of this article were defrayed in part by the payment of page charges. This article must therefore be hereby marked *advertisement* in accordance with 18 U.S.C. Section 1734 solely to indicate this fact.

Requests for reprints: Takayuki Ikezoe, Department of Internal Medicine, Kochi Medical School, Nankoku, Kochi, 783-8505, Japan. Phone: 81-88-880-2345; Fax: 81-88-880-2348; E-mail: ikezoet@med.kochi-ms.ac.jp.

One microgram of DNase I-treated RNA was reverse transcribed by using Moloney murine leukemia virus reverse transcriptase (Life Technologies, Inc.), and 50 ng of the resulting complementary DNAs (cDNAs) were used as templates for PCR. Real-time PCR was carried out by using TaqDNA polymerase (Qiagen, Valencia, CA), 50 ng cDNA for *CYP3A4* (500–5 ng in serial dilutions for standard curves), or 1 pg for *18S* (10–0.1 pg for standard curve), and SYBR Green I nucleic acid gel staining solution in a 1:60,000 dilution. Primers used for *CYP3A4* were 5′-CCTGAGAAGTTCCTCCCTGA-3′ and 5′-AATGCAGTTTCTGGGTCCAC-3, which yielded a 99-bp product. PCR conditions were as follows: a 95°C initial activation for 15 minutes followed by 45 cycles of 95°C for 15 seconds, 60°C for 15 seconds, and 72°C for 30 seconds, and fluorescence determination at the melting temperature of the product for 20 seconds on an ICycler detection system (Bio-Rad, Hercules, CA). We measured expression of *18S* for normalization.

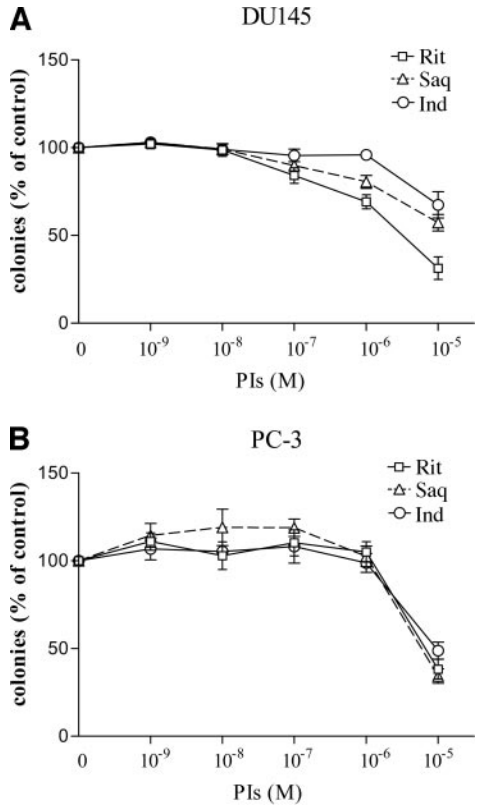

Fig. 1. Dose-response activity of ritonavir, saquinavir, and indinavir on clonal proliferation of DU145 (*A*) and PC-3 (*B*) androgen-independent prostate cancer cells. DU145 (*A*) and PC-3 (*B*) cells (500 cells/plate) were cultured with a variety of concentrations of PIs (10^{-9} to 10^{-5} mol/L). Colonies (>40) were enumerated after 14 days of incubation. Results are expressed as a mean percentage of control plates containing 0.1% DMSO (control diluent). Each point represents a mean of three independent experiments with triplicate plates. *Bars*, SD; *Rit*, ritonavir; *Saq*, saquinavir; *Ind*, indinavir.

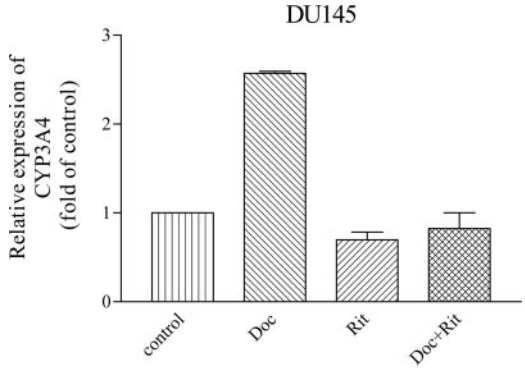

Fig. 3. Effect of ritonavir on docetaxel-induced expression of *CYP3A4* transcripts in DU145 cells. Cells were cultured for 24 hours with docetaxel (10^{-9} mol/L), ritonavir (10^{-5} mol/L), or both. RNA was extracted, and cDNA was synthesized and subjected to real-time PCR to measure the level of *CYP3A4*. Data represent mean ± SD of triplicate cultures. *Doc*, docetaxel; *Rit*, ritonavir.

Western Blot Analysis. DU145 cells (10^5/mL) were incubated with a variety of concentrations of docetaxel (10^{-9} to 10^{-6} mol/L) and ritonavir (10^{-5} mol/L) either alone or in combination for 24 hours in six-well plates. Lysates were made by standard methods as described previously (14). Protein concentrations were quantitated using a Bio-Rad assay. Proteins were resolved on a 4% to 15% SDS polyacrylamide gel, transferred to an Immobilon polyvinylidene difluoride membrane (Amersham Corp., Piscataway, NJ), and probed sequentially with antibodies. Anti-poly(ADP-ribose) polymerase (PARP; Santa Cruz Biotechnology, Santa Cruz, CA), caspase-3 (Santa Cruz Biotechnology), and β-actin (Santa Cruz Biotechnology) antibodies were used. The band intensities were measured using densitometry.

Transient Transfection of NFκB Small Interfering RNA. DU145 cells were transiently transfected with NFκB small interfering RNA (siRNA; final concentration of 100 nmol/L) using Signalsilence siRNA kit (Cell Signaling Technology, Beverly, MA) according to manufacturer's instruction. Following

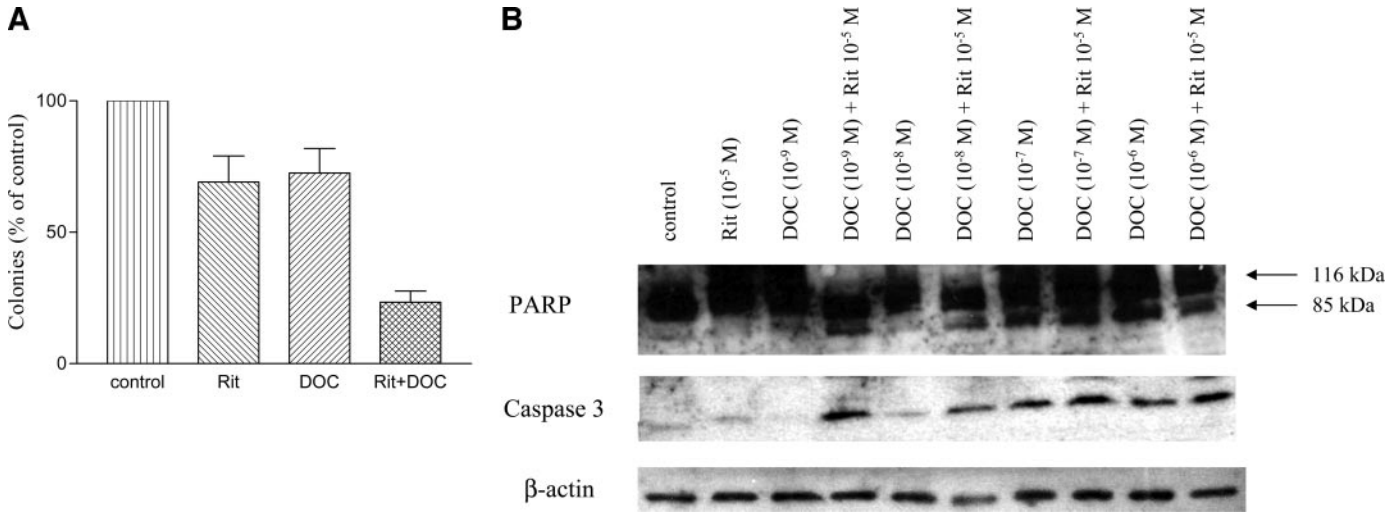

Fig. 2. Effect of ritonavir on growth arrest and apoptosis mediated by docetaxel. *A*, clonal assay. DU145 cells were cultured with docetaxel (10^{-10} mol/L), ritonavir (10^{-6} mol/L), or both. Colonies (>40) were enumerated after 14 days of incubation. Results are expressed as a mean percentage of control plates containing 0.1% DMSO (control diluent). Each point represents a mean of three independent experiments with triplicate plates; *bars*, SD. *B*, Western blot analysis. DU145 cells were cultured with docetaxel (10^{-9} to 10^{-6} mol/L), ritonavir (10^{-5} mol/L), or the combination of both for 4 days. Cells were harvested and subjected to Western blot analysis. The polyvinylidene fluoride membrane was sequentially probed with anti–caspase-3, PARP, and β-actin antibodies. *Rit*, ritonavir; *Doc*, docetaxel.

transfection, DU145 cells were subjected to Western blot analysis and MTT assay in the presence or absence of docetaxel.

Evaluation of NFκB activity by ELISA. The DNA binding activity of NFκB in prostate cancer cells was quantified by ELISA using the *trans*-AM NFκB p65 Transcription Factor Assay kit (Active Motif North America, Carlsbad, CA), according to the instructions of the manufacturer. Briefly, nuclear extracts were prepared as described previously and incubated in 96-well plates coated with immobilized oligonucleotide (5′-AGTTGAGGGGACTTTCCCAGGC-3′) containing a consensus (5′-GGGACTTTCC-3′) binding site for the p65 subunit of NFκB. NFκB binding to the target oligonucleotide was detected by incubation with primary antibody specific for the activated form of p65 (Active Motif North America), visualized by anti-IgG horseradish peroxidase conjugate and developing solution, and quantified at 450 nm with a reference wavelength of 655 nm. Background binding was subtracted from the value obtained for binding to the consensus DNA sequence.

Mice. Twenty male triple immunodeficient BNX *nu/nu* mice at 8 weeks of age were purchased from Harlan Sprague Dawley Inc. (Indianapolis, NJ) and were maintained in pathogen-free conditions with irradiated chow.

Treatment Protocol. Animals were bilaterally, subcutaneously injected with 2×10^6 DU145 cells/tumor in 0.1 mL Matrigel (Collaborative Biomedical Products, Bedford, MA). Mice were divided randomly into four groups of five mice each: group A, control diluent (control); group B, ritonavir; group C, docetaxel; and group D, docetaxel + ritonavir. Ritonavir (10 mg/kg/mouse) was administered five times a week orally. Docetaxel (25 mg/kg/mouse) was administered intravenously once a week. The dose of ritonavir and docetaxel was determined by our preliminary studies. Tumors were measured every week with vernier calipers. Tumor size was calculated by the formula: $a \times b \times c$, where "a" is the length and "b" is the width and "c" is the height in millimeters. At the end of the experiment, animals were sacrificed by CO_2 asphyxiation, and tumor weights were measured after their careful resection. Blood also was collected from the orbital sinus for chemistry and hematopoietic analysis.

Histology. Tumors were fixed for 12 hours in 10% neutral buffered formaldehyde after sacrifice; tissue blocks were embedded in paraffin; and H&E-stained sections were examined by light microscopy.

Statistical Analysis. The statistical significance of the differences was analyzed using the nonparametric Mann-Whitney *U* test.

RESULTS

Effect of PIs on Clonal Proliferation of Androgen-Independent Prostate Cancer Cells. The DU145 and PC-3 prostate cancer cells were cloned in soft agar in the presence of various concentrations of

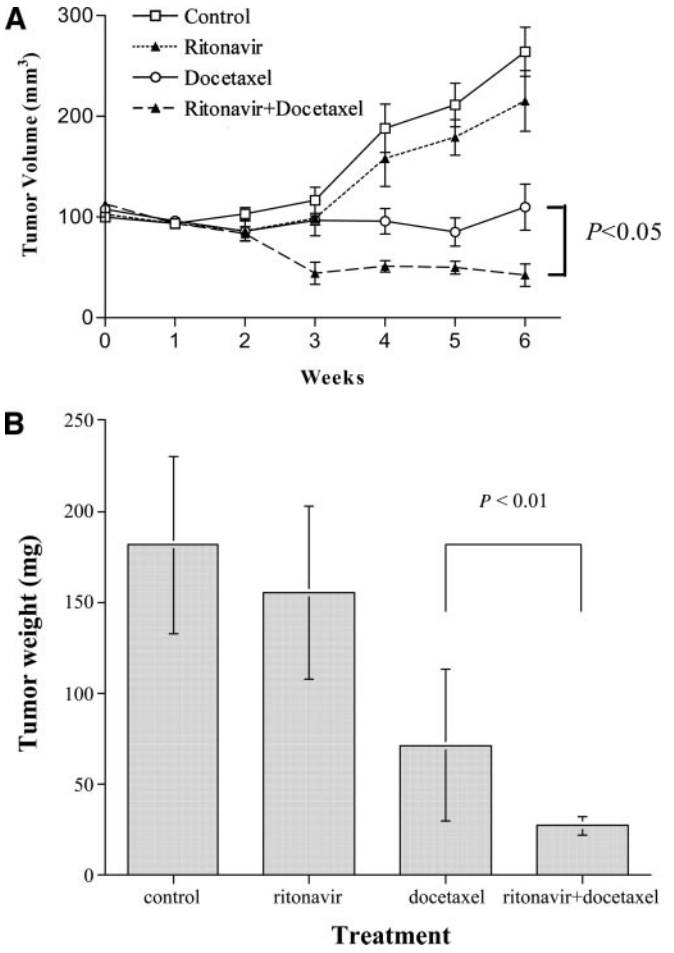

Fig. 5. Effect of ritonavir, docetaxel, or both on growth of DU145 tumors in BNX triple-immunodeficient mice. *A.* DU145 cells were injected bilaterally subcutaneously into BNX mice, forming two tumors/mouse. Ritonavir (10 mg/kg/mouse), docetaxel (25 mg/kg/mouse), and the combination of both were administered to mice for 5 days a week for 6 weeks. Tumor volumes were measured every week. Each point represents the mean ± SD of 10 tumors. *B,* tumor weights at autopsy. After 6 weeks of treatment, tumors were removed and weighed. Results represent mean ± SD of tumor weights. Statistical significance was determined by Mann-Whitney *U* test; *bars,* SD.

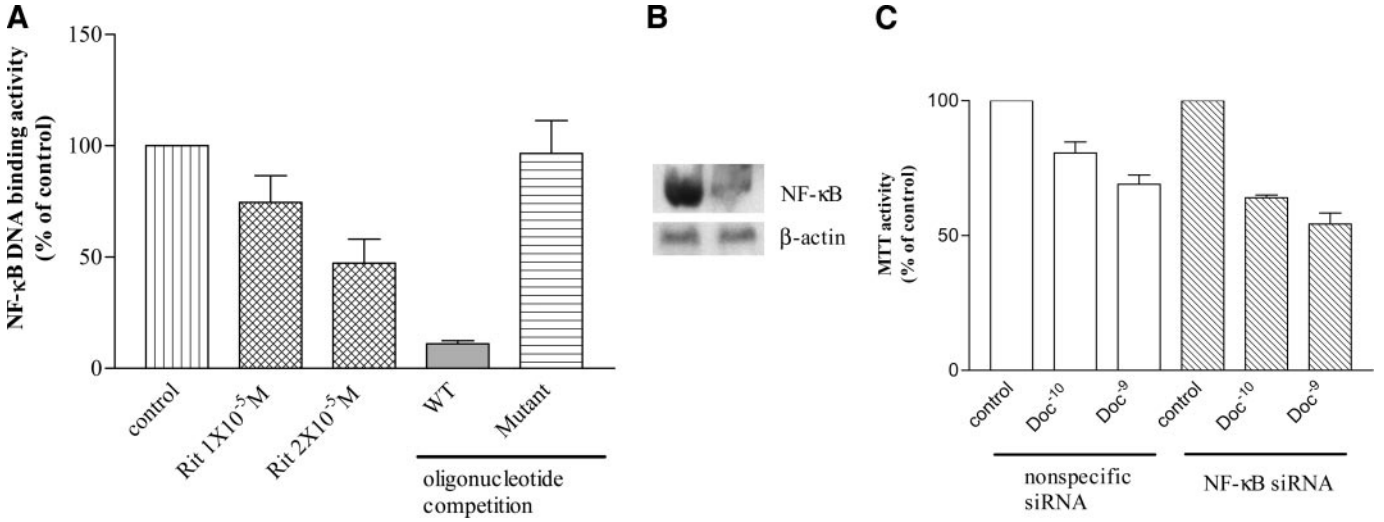

Fig. 4. Effect of ritonavir on NFκB/DNA binding activity in DU145 cells. *A,* ELISA. DU145 cells were plated in six-well plates and cultured either with or without ritonavir (1 or 2×10^{-5} mol/L) for 48 hours; nuclear protein was extracted and subjected to ELISA for measurement of NFκB/DNA binding activity. Results represent the mean ± SD of two experiments done in duplicate. Cold competition was performed using either wild-type NFκB DNA binding oligonucleotides (*WT*) or mutated NFκB DNA binding oligonucleotides (*Mutant*). *Rit,* ritonavir. *B,* transient transfection of NFκB siRNA. DU145 cells were transiently transfected with either NFκB siRNA or nonspecific siRNA. After 2 days, cells were harvested, and proteins were extracted and subjected to Western blot analysis. Membrane was probed sequentially with antibodies against Akt and *β*-actin. The blots were developed using the enhanced chemiluminescence kit. *B,* MTT assay. After 2 days of transfection, the control and NFκB siRNA-transfected DU145 cells were plated in 96-well plates and cultured either with or without docetaxel. On the third day of culture, the cell numbers and viability were evaluated by MTT assay.

PIs (10^{-9} to 10^{-5} mol/L). Dose-response curves were drawn, and the ED_{50} that inhibited colony formation was determined. Each of the three PIs—ritonavir, saquinavir, and indinavir—was effective at inhibiting clonal proliferation of the DU145 and PC-3 cells in a dose-dependent manner (Fig. 1*A* and *B*). The most effective PI was ritonavir, which caused a 50% decrease clonal growth of DU145 cells at 3×10^{-6} mol/L (Fig. 1*A*). Ritonavir and saquinavir showed nearly equivalent potency against PC-3 cells with an ED_{50} of 8×10^{-6} mol/L (Fig. 1*B*). Conversely, none of PIs inhibited growth of normal myeloid committed stem cells (CFU-GM) in soft agar containing cytokines including interleukin 3 and granulocyte macrophage-colony stimulating factor even at a high concentration of PI (2×10^{-5} mol/L; data not shown).

Ritonavir Enhances Growth Arrest and Apoptosis Mediated by Docetaxel. The DU145 cells were cultured with docetaxel (10^{-10} mol/L) either alone or in combination with ritonavir (10^{-6} mol/L) to evaluate the effect of the combinations of these drugs. Docetaxel (10^{-10} mol/L) inhibited the growth of DU145 cells by 28 ± 9%, and ritonavir (10^{-6} mol/L) inhibited proliferation by 30 ± 9%. The combination of docetaxel (10^{-10} mol/L) and ritonavir (10^{-6} mol/L) decreased the growth of DU145 cells by 77 ± 4% (Fig. 2*A*).

Further studies investigated whether ritonavir enhanced the pro-apoptotic effect of docetaxel in DU145 cells using Western blot analysis to detect cleavage of PARP, which is a target of caspases. The cleavage of PARP is thought to be a late event in apoptosis. Docetaxel (10^{-9} to 10^{-6} mol/L) cleaved PARP because caspase-3 was activated in a dose-dependent manner (Fig. 2*B*). Ritonavir (10^{-5} mol/L) potentiated the effects of docetaxel to activate caspase-3 and cleave its target molecule PARP (Fig. 2*B*). For example, the activated form of caspase-3 and cleaved PARP were negligible in DU145 cells treated with docetaxel (10^{-9} mol/L) alone; however, the combination of docetaxel (10^{-9} mol/L) and ritonavir (10^{-5} mol/L) induced activation of caspase-3 and cleavage of PARP in DU145 cells.

Effect of Ritonavir on Docetaxel-Induced Expression of *CYP3A4* Transcripts. The level of *CYP3A4* transcripts in DU145 cells was measured using real-time PCR. DU145 cells constitutively expressed *CYP3A4*, and docetaxel (10^{-9} mol/L, 24 hours) increased its expression by 2.5-fold (Fig. 3). Ritonavir (10^{-5} mol/L, 24 hours) completely blocked this induction (Fig. 3). These data suggested that ritonavir inhibited the ability of docetaxel to induce expression of *CYP3A4* at the transcriptional level.

Effect of Ritonavir on DNA Binding Activity of NFκB in DU145 Cells. NFκB stimulates cell proliferation and confers cellular resistance to chemotherapy (15–18). Therefore, NFκB can be a molecular target of cancer treatment. The effect of ritonavir on NFκB activity was explored using an ELISA-based assay. Control DU145 cells possessed strong NFκB/DNA binding activity (data not shown). Treatment of DU145 cells with ritonavir (1 or 2×10^{-5} mol/L) inhibited the NFκB binding activity by either 25 ± 7% or 53 ± 13%, respectively, as compared with untreated control cells (Fig. 4*A*). As control, 100-fold molar excess of the wild-type NFκB consensus oligonucleotides was added to the assay of control lysate from untreated cells. Binding was inhibited by at least 80%; however, mutated NFκB consensus oligonucleotides at the same molar excess were unable to inhibit binding (Fig. 4*A*), ascertaining the specificity of binding of NFκB to its consensus binding site.

Inhibition of NFκB by siRNA Augmented Cytotoxicity of Docetaxel. To explore whether inhibition of NFκB sensitizes DU145 cells to the antitumor effect of docetaxel, DU145 cells were transiently transfected with either NFκB siRNA or control siRNA. After 48 hours, cells were harvested and subjected to Western blot analysis, showing that NFκB siRNA effectively down-regulated levels of this transcription factor (Fig. 4*B*). Transfectants were cultured either with or without docetaxel for another 48 hours and subjected to MTT assay. NFκB siRNA-transfected DU145 cells were more sensitive to growth inhibition mediated by docetaxel compared with nonspecific siRNA-transfected cells (Fig. 4*C*). For example, 10^{-10} mol/L docetaxel inhibited growth of control cells by 20%; however, it inhibited growth of NFκB siRNA-transfected cells by 34% ($P < 0.005$) under similar culture conditions (Fig. 4*C*).

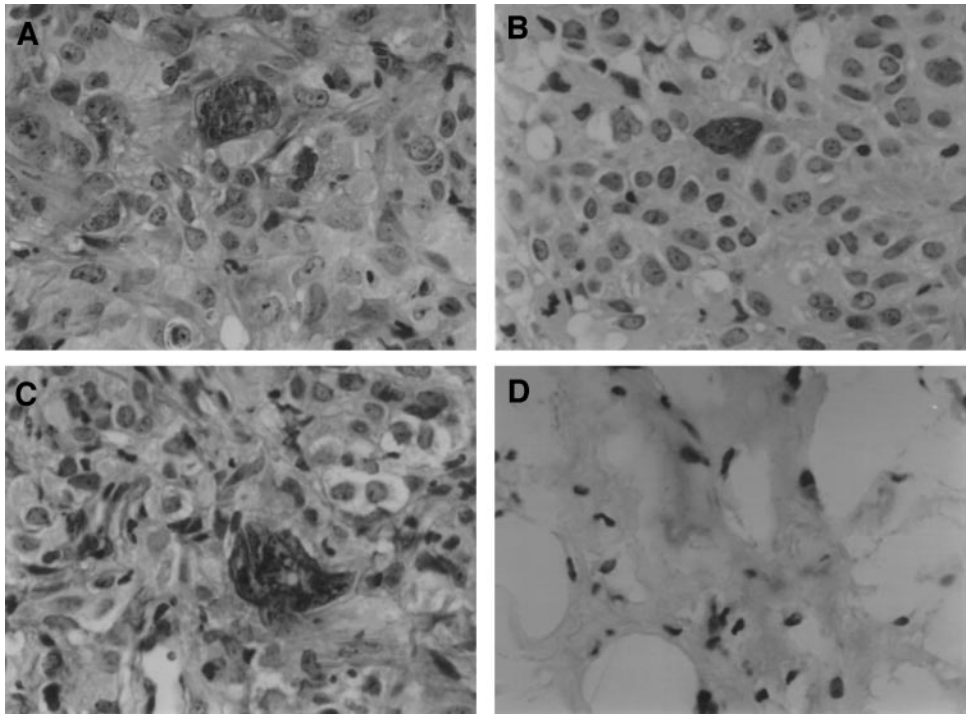

Fig. 6. Antitumor effect of ritonavir, docetaxel, or the combination of both *in vivo*. After 6 weeks of therapy with ritonavir and docetaxel either alone or in combination (as described in Fig. 5), tumors were removed from BNX triple-immunodeficient mice, fixed, and stained (H&E). *A*, DU145 control tumor has poorly differentiated carcinoma cells without necrosis (original ×200). *B*, DU145 tumors from mice treated with ritonavir (10 mg/kg/day) for 6 weeks. The histology appears similar to control tumors (*A*; original ×200). *C*, DU145 tumors from mice treated with docetaxel (25 mg/kg/day) for 6 weeks. Portions of the tumor show tumor necrosis (original ×200). *D*, DU145 tumors from mice treated with the combination of ritonavir (10 mg/kg/day) and docetaxel (25 mg/kg/day) for 6 weeks show extensive tumor necrosis and fibrotic changes (original ×200).

Ritonavir Increased the Antitumor Activity of Docetaxel *In vivo*. We evaluated the ability of ritonavir to enhance the ability of docetaxel to inhibit the growth of AIPC DU145 cells growing as xenografts in male BNX *nu/nu* triple immunodeficient mice. One day after injection of DU145 cells, mice were treated with ritonavir, docetaxel, or both. Control mice received diluent alone. Tumor volume was measured every week (Fig. 5*A*), and tumor weights were determined at autopsy (Fig. 5*B*). Docetaxel markedly suppressed the growth and weights of DU145 tumors. No statistical significance was noted in either the size or weights of the DU145 tumors in the mice that received ritonavir alone as compared with the control mice; however, the combination of ritonavir and docetaxel significantly decreased the size ($P = 0.05$) of DU145 tumors compared with mice that received docetaxel alone (Fig. 5*A*). The difference of mean tumor weights between these two groups was even more significant (Fig. 5*B*; $P < 0.01$). The tumors from mice that received docetaxel alone weighed 72 ± 41 mg. Conversely, tumors from mice that received the combination of docetaxel and ritonavir weighed only 27 ± 5 mg (Fig. 5*B*).

The tumors and organs of the mice were fixed, stained, and viewed by light microscopy. The tumors from control mice showed typical histologic appearance of infiltrating, poorly differentiated adenocarcinomas of the prostate (Fig. 6*A*). The mice that received ritonavir alone showed a similar histologic appearance as the control mice (Fig. 6*B*). The histologic analysis of the tumors from mice treated with docetaxel alone showed necrotic tissue with ~40% of cancer cells undergoing necrosis (Fig. 6*C*). Cancer cells were not found in the mice that received the combination of docetaxel and ritonavir; the site of tumor was composed of necrotic and fibrotic tissues (Fig. 6*D*). Organs from mice treated with the various therapies did not show any changes compared with controls, including their liver, kidney, spleen, bone marrow, lung, and heart. During the study, all of the mice were weighed each week; the mean weights of each of the experimental groups were statistically the same as those of the control mice (data not shown). Blood analyses were performed several hours before the mice were sacrificed. No difference in the mean hematopoietic values and blood chemistries was observed between treated and untreated mice (data not shown).

The ability of ritonavir to enhance antitumor effects of docetaxel also was studied using established DU145 xenografts (Fig. 7). Once tumor volume reached approximately a mean of 200 mm^3, treatment was initiated. Ritonavir again significantly enhanced the ability of docetaxel to decrease tumor size ($P = 0.01$) and tumor weight ($P = 0.008$) of DU145 xenografts (Fig. 7*A* and *B*). We measured apoptosis of DU145 tumor cells using terminal deoxynucleotidyl transferase-mediated nick end labeling (TUNEL) assay. TUNEL-positive cells were negligible in control and ritonavir-treated mice. Conversely, docetaxel induced ~8% of DU145 cells to become TUNEL positive. Importantly, when docetaxel was combined with ritonavir, TUNEL-positive cells increased to 16% (data not shown). At the end of this experiment, we sacrificed the mice, removed their tumors, extracted RNA, and measured levels of *CYP3A4* by real-time PCR. At 16 hours before sacrifice, either docetaxel or ritonavir alone or in combination was administered to the mice. As shown in Fig. 7*C*, docetaxel increased expression of *CYP3A4* by approximately twofold in DU145 tumors; when docetaxel was combined with ritonavir, docetaxel-induced expression of CYP3A4 was blocked completely. We also extracted nuclear protein from tumors and explored the effect of ritonavir on NFκB DNA binding activity (Fig. 7*D*). Control tumors possessed measurable NFκB DNA binding activity (mean absorbance at 450 mm, 0.73 ± 0.15), and ritonavir inhibited this activity by 40% (mean absorbance at 450 mm, 0.43 ± 0.1). These results were consistent with those obtained from the *in vitro* studies (Figs. 3 and 4).

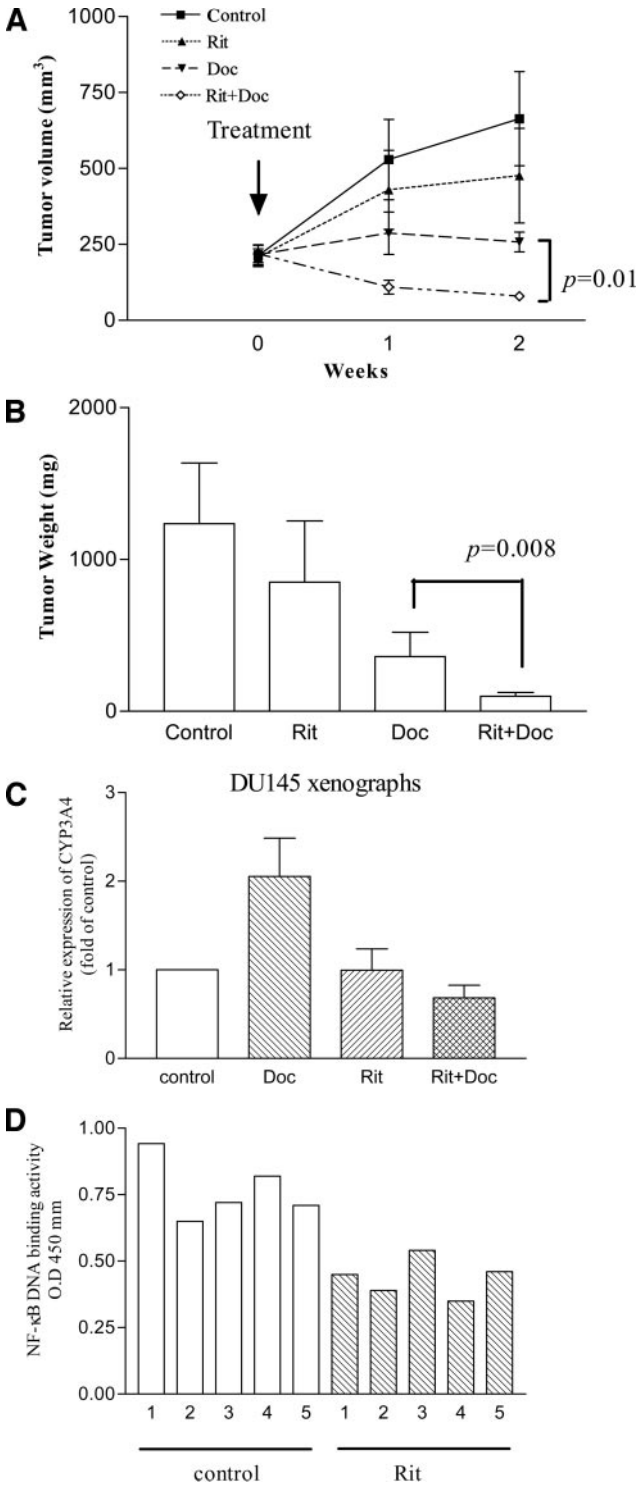

Fig. 7. Effect of ritonavir, docetaxel, or the combination of both against established DU145 xenografts. DU145 cells were injected bilaterally subcutaneously into BNX mice, forming two tumors/mouse. When tumor volume reached ~200 mm^3, mice were randomized into five groups ($n = 5$ each), and treatment was initiated with ritonavir (10 mg/kg/mouse), docetaxel (25 mg/kg/mouse), or the combination of both for 5 days a week for 2 weeks. Tumor volumes were measured every week. Each point represents the mean ± SD of 10 tumors. *B*, tumor weights at autopsy. After 2 weeks of treatment, tumors were removed and weighed. Results represent mean ± SD of tumor weights. Statistical significance was determined by Mann-Whitney *U* test; *bars*, SD. *C*, effect of ritonavir on docetaxel-induced expression of *CYP3A4* transcripts *in vivo*. After 16 hours of drug administration, tumors were removed, RNA was extracted, and cDNA was synthesized. Real-time PCR was performed to measure the level of *CYP3A4*. Data represent mean ± SD of three tumors. *Doc*, docetaxel; *Rit*, ritonavir. *D*, Effect of ritonavir on NFκB DNA binding activity *in vivo*. After 16 hours of drug administration, tumors were removed, and nuclear protein was extracted and subjected to ELISA to measure NFκB DNA binding activity. *Rit*, ritonavir; *O.D.*, optical density.

DISCUSSION

The HIV-1 PI, ritonavir, blocked docetaxel-induced expression of *CYP3A4* in AIPC DU145 cells *in vitro* and *in vivo*. Thus, ritonavir probably protected docetaxel from inactivation in DU145 cells, resulting in increased intracellular levels and enhanced antitumor effects. Xenobiotics, including anticancer drugs such as docetaxel, bind to steroid and xenobiotic receptor. Ligand-activated steroid and xenobiotic receptor forms heterodimer with retinoid X receptor and binds to the promoter region of the *CYP3A4* gene and activates its transcription (19, 20). Recent studies showed that coregulators, including silencing mediator for retinoid and thyroid receptor and steroid receptor coactivator-1, mediated basal and xenobiotic-induced transcriptional activity of *CYP3A4* (20). The investigators found that the antifungal agent ketoconazole inhibited corticosterone-induced *CYP3A4* transcriptional activity by interacting with these coregulators (20). Ritonavir may block docetaxel-induced expression of *CYP3A4* by also affecting these coregulators. Further studies clearly will be needed to elucidate molecular mechanism by which ritonavir inhibits docetaxel-induced expression of *CYP3A4*.

P-gp is an integral plasma membrane protein encoded by the multidrug-resistant (*MDR*) gene belonging to the ATP-binding cassette family of transporters (21). It is an energy-dependent efflux pump for a wide variety of compounds, including anticancer drugs such as docetaxel (15). The cancer cells from individuals with advanced, refractory cancers, including prostate, breast, and lung, overexpress P-gp transcripts (22, 23). Thus, overexpression of P-gp is considered to contribute to drug resistance. Ritonavir was shown to inhibit the activity of P-gp; thus, ritonavir also might enhance the activity of docetaxel by blocking its cellular efflux, although PIs, including ritonavir, also are substrate for P-gp (24, 25). We and other investigators found that P-gp–overexpressing doxorubicin-resistant breast cancer MCF-7 cells were resistant to docetaxel (data not shown; ref. 26). Our preliminary studies showed that ritonavir enhanced the ability of docetaxel to decrease the growth of these cells (data not shown).

Recent studies found that PIs inhibited 26S proteasome activity. Ritonavir and saquinavir inhibited the degradation of IκBα, which prevented the nuclear translocation and transcriptional activation of NFκB in Kaposi sarcoma and prostate cancer cells (5, 7). This was associated with growth arrest and apoptosis of these cells. Cancer cells including prostate cancer often have hyperactivity of the NFκB pathway, which can make these malignant cells relatively resistant to chemotherapy (16–18). In this study, we have found that DU145 cells possessed strong NFκB DNA binding activity, and ritonavir decreased this activity *in vitro* (Fig. 4*A*) and *in vivo* (Fig. 7*D*). This also may contribute to the increased cytotoxicity of the combination of ritonavir and docetaxel.

In summary, we suggest a novel approach to cancer therapy by using an active chemotherapeutic drug and a PI (ritonavir) to help reverse the mechanisms of drug resistance, including rapid drug metabolism, efficient removal of the drug from the target cancer cells, and down-regulation of the NFκB pathway.

REFERENCES

1. Beer TM, Pierce WC, Lowe BA, Henner WD. Phase II study of weekly docetaxel in symptomatic androgen-independent prostate cancer. Ann Oncol 2001;12:1273–9.
2. Picus J, Schultz M. Docetaxel (Taxotere) as monotherapy in the treatment of hormone-refractory prostate cancer: preliminary results. Semin Oncol 1999;17:14–8.
3. Friedland D, Cohen J, Miller R Jr, et al. A phase II trial of docetaxel (Taxotere) in hormone-refractory prostate cancer: correlation of antitumor effect to phosphorylation of Bcl-2. Semin Oncol 1999;17:19–23.
4. Ikezoe T, Daar ES, Hisatake J, Taguchi H, Koeffler HP. HIV-1 protease inhibitors decrease proliferation and induce differentiation of human myelocytic leukemia cells. Blood 2000;96:3553–9.
5. Pati S, Pelser CB, Dufraine J, Bryant JL, Reitz MS Jr, Weichold FF. Antitumorigenic effects of HIV protease inhibitor ritonavir: inhibition of Kaposi sarcoma. Blood 2002;99:3771–9.
6. Sgadari C, Barillari G, Toschi E, et al. HIV protease inhibitors are potent anti-angiogenic molecules and promote regression of Kaposi sarcoma. Nat Med 2002;8: 225–32.
7. Pajonk F, Himmelsbach J, Riess K, Sommer A, McBride WH. The human immunodeficiency virus (HIV)-1 protease inhibitor saquinavir inhibits proteasome function and causes apoptosis and radiosensitization in non-HIV-associated human cancer cells. Cancer Res 2002;62:5230–5.
8. Ikezoe T, Saito T, Bandobashi K, Yang Y, Koeffler HP, Taguchi H. HIV-1 protease inhibitor induces growth arrest and apoptosis of human multiple myeloma cells via inactivation of signal transducer and activator of transcription 3 and extracellular signal-regulated kinase 1/2. Mol Cancer Ther 2004;3:473–9.
9. Kumar GN, Rodrigues AD, Buko AM, Denissen JF. Cytochrome P450-mediated metabolism of the HIV-1 protease inhibitor ritonavir (ABT-538) in human liver microsomes. J Pharmacol Exp Ther 1996;277:423–31.
10. Kempf DJ, Marsh KC, Kumar G, et al. Pharmacokinetic enhancement of inhibitors of the human immunodeficiency virus protease by coadministration with ritonavir. Antimicrob Agents Chemother 1997;41:654–60.
11. Washington CB, Flexner C, Sheiner LB, et al. AIDS Clinical Trials Group Protocol (ACTG 378) Study Team. Effect of simultaneous versus staggered dosing on pharmacokinetic interactions of protease inhibitors. Clin Pharmacol Ther 2003;73:406–46.
12. Cvetkovic RS, Goa KL. Lopinavir/ritonavir: a review of its use in the management of HIV infection. Drugs 2003;63:769–802.
13. Royer I, Monsarrat B, Sonnier M, Wright M, Cresteil T. Metabolism of docetaxel by human cytochromes P450: interactions with paclitaxel and other antineoplastic drugs. Cancer Res 1996;56:58–65.
14. Ikezoe T, Miller CW, Kawano S, et al. Mutational analysis of the peroxisome proliferator-activated receptor γ gene in human malignancies. Cancer Res 2001;61:5307–10.
15. Bardelmeijer HA, Ouwehand M, Buckle T, et al. Low systemic exposure of oral docetaxel in mice resulting from extensive first-pass metabolism is boosted by ritonavir. Cancer Res 2002;62:6158–64.
16. Suh J, Payvandi F, Edelstein LC, et al. Mechanisms of constitutive NF-κB activation in human prostate cancer cells. Prostate 2002;52:183–200.
17. Ma MH, Yang HH, Parker K, et al. The proteasome inhibitor PS-341 markedly enhances sensitivity of multiple myeloma tumor cells to chemotherapeutic agents. Clin Cancer Res 2003;9:1136–44.
18. Huang Y, Johnson KR, Norris JS, Fan W. Nuclear factor-κB/IκB signaling pathway may contribute to the mediation of paclitaxel-induced apoptosis in solid tumor cells. Cancer Res 2000;60:4426–32.
19. Xie W, Barwick JL, Downes M, et al. Humanized xenobiotic response in mice expressing nuclear receptor SXR. Nature 2000;406:435–9.
20. Takeshita A, Taguchi M, Koibuchi N, Ozawa Y. Putative role of the orphan nuclear receptor SXR (steroid and xenobiotic receptor) in the mechanism of CYP3A4 inhibition by xenobiotics. J Biol Chem 2002;277:32453–8.
21. Gottesman MM, Hrycyna CA, Schoenlein PV, Germann UA, Pastan I. Genetic analysis of the multidrug transporter. Annu Rev Genet 1995;29:607–49.
22. Van Brussel JP, Jan Van Steenbrugge G, Van Krimpen C, et al. Expression of multidrug resistance related proteins and proliferative activity is increased in advanced clinical prostate cancer. J Urol 2001;165:130–5.
23. Gottesman MM, Fojo T, Bates SE. Multidrug resistance in cancer: role of ATP-dependent transporters. Nat Rev Cancer 2002;2:48–58.
24. Lee CG, Gottesman MM, Cardarelli CO, et al. HIV-1 protease inhibitors are substrates for the MDR1 multidrug transporter. Biochemistry 1998;37:3594–601.
25. Olson DP, Scadden DT, D'Aquila RT, De Pasquale MP. The protease inhibitor ritonavir inhibits the functional activity of the multidrug resistance related-protein 1 (MRP-1). AIDS 2002;16:1743–7.
26. Ciardiello F, Caputo R, Borriello G, et al. ZD1839 (IRESSA), an EGFR-selective tyrosine kinase inhibitor, enhances taxane activity in bcl-2 overexpressing, multidrug-resistant MCF-7 ADR human breast cancer cells. Int J Cancer 2002;98:463–9.